Imbibition in geometries with axial variations

MATHILDE REYSSAT, LAURENT COURBIN, ETIENNE REYSSAT AND HOWARD A. STONE

School of Engineering and Applied Sciences, Harvard University, Cambridge, MA 02138, USA

When surface wetting drives liquids to invade porous media or microstructured materials with uniform channels, the penetration distance is known to increase as the square root of time. We demonstrate, experimentally and theoretically, that shape variations of the channel, in the flow direction, modify this 'diffusive' response. At short times, the shape variations are not significant and the imbibition is still diffusive. However, at long times, different power-law responses occur, and their exponents are uniquely connected to the details of the geometry. Experiments performed with conical tubes clearly show the two theoretical limits. Several extensions of these ideas are described.

1. Introduction

The quasi-steady movement of liquids through capillary tubes, due to the wetting of the liquid on the walls, was described a century ago (see Bell & Cameron 1906; Lucas 1918; Washburn 1921): for a capillary tube of constant section, the position of the meniscus obeys diffusive dynamics $\ell^2 = Dt$, where ℓ represents the distance through which the liquid has moved in the time t and D is a coefficient that depends on the characteristics of the tube and the liquid. This robust result, often casually referred to as 'Washburn's law', also applies, at least approximately, to the dynamics of imbibition of porous media such as filter paper, packed beds of granular materials, dry soils (see Dullien 1979), as well as microtextured surfaces (see Bico, Tordeux & Quéré 2001; Courbin *et al.* 2007), etc.

Numerous studies on this topic of capillary invasion have been performed, including investigations of the influence of the geometry of the channels: the shape of a uniform cross-section (see Krotov & Rusanov 1999; Polzin & Choueiri 2003), the stepped capillary tube, i.e. a succession of different but uniform cross-sections (see Erickson, Li & Park 2002; Polzin & Choueiri 2003; Young 2004) and V-shaped open grooves (see Romero & Yost 1996; Rye, Yost & O'Toole 1998; Weislogel & Lichter 1998; Dussaud, Adler & Lips 2003; Warren 2004). But, to the best of our knowledge, all of these studies concern, at least locally (for the stepped capillary tube geometry) or totally, channels with uniform cross-sections.

In this paper we consider structured porous media that have a systematic and monotonic shape change and find that at short times the capillary-driven invasion is diffusive as described above, but that at longer times $\ell \propto t^\beta$, where the scaling exponent $\beta \neq 1/2$ and is a function of the shape of the gap along which the flow occurs. The theoretical analysis developed in §2 is compared with experimental data obtained with a conical geometry in §3. In §4, we extend our analysis to other geometries. We conclude in §5 where we also indicate often neglected early papers in this literature.
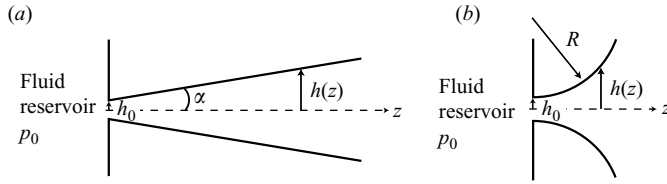
FIGURE 1. Different geometries for illustrating variants of the capillary-driven invasion of a structured porous solid with axial shape variations: (*a*) conical and (*b*) parabolic channels or tubes. We denote by α half of the opening angle in geometry (*a*) and by R the radius of curvature in geometry (*b*). In both cases, h_0 and $h(z)$ are, respectively, half of the width (in two dimensions) or the radius of the tube (in three dimensions), at the opening and at the distance z. The pressure of the reservoir of liquid is p_0.

2. Generalization of one-dimensional capillary invasion

We study the influence of the channel geometry on the imbibition dynamics. We treat the incompressible flows as one-dimensional in the axial or z-direction, while using the classical Darcy description to characterize the viscously dominated dynamics. We present simultaneously results for the two-dimensional and the three-dimensional axisymmetrical geometries and consider the specific configurations shown in figure 1. The analytic development, however, is general for any one-dimensional flow to which the Darcy description applies. For example, in figure 1(*a*) we denote by $h(z)$ half of the width of a wedge-shaped channel (two dimensions) or the radius of a conically shaped tube (three dimensions); $z = 0$ indicates the location of the opening. More generally, the geometry may vary as in figure 1(*b*). When estimating the permeability k in the analyses below we use estimates based on the lubrication approximation ($|\mathrm{d}h/\mathrm{d}z| \ll 1$). These channels are in contact with a reservoir of liquid at ambient pressure p_0, and wetting of the liquid on the walls leads to an invasion process.

The average velocity $u(z, t)$ is assumed to be in the form of Darcy's law,

$$\frac{\mu u}{k} = -\frac{\partial p}{\partial z}, \qquad (2.1)$$

where $k(z)$ is the permeability, which depends on the detailed shape of the cross-section, μ is the viscosity of the liquid and the pressure gradient changes in time during the imbibition process. For slowly varying nearly rectangular shapes $k = h^2/\lambda$, where $\lambda = 3$ in two-dimensional and $\lambda = 8$ for axisymmetric three-dimensional geometries (assuming that the cross-sectional geometry is narrow). In addition, a one-dimensional mass conservation statement requires $2uh = q(t)$ in two dimensions, where $q(t)$ is the volumetric flow rate per unit width, or $\pi u h^2 = Q(t)$ in three dimensions, where $Q(t)$ is the volumetric flow rate.

We further assume that the fluid mostly wets the solid and that the meniscus is at position $z = \ell(t)$. We aim to determine $\ell(t)$, which in the case of a uniform shape yields the traditional description with $\ell \propto t^{1/2}$. At the meniscus, the pressure in the invading liquid is $p = p_0 - \gamma \kappa$, where γ is the surface tension of the liquid and the curvature of the interface κ is proportional to $1/h$. Thus, we write the liquid pressure at the meniscus as $p = p_0 - c\gamma/h$, where c depends on the local geometry and the contact angle the liquid makes with the solid. For the clarity of our calculations, we choose to detail both the two-dimensional (2D) and the three-dimensional (3D) cases and not to give a general formula valid for both. Thus, combining the Darcy and

continuity equations yields

$$\frac{3\mu q(t)}{2h(z)^3} = -\frac{\partial p}{\partial z} \quad \text{(2D)} \quad \text{or} \quad \frac{8\mu Q(t)}{\pi h(z)^4} = -\frac{\partial p}{\partial z} \quad \text{(3D)}. \tag{2.2}$$

These equations may be integrated between $z = 0$ (where $p = p_0$) and the location of the meniscus ($z = \ell(t)$ where the opening has half-height $h(\ell(t))$). Thus, we find the flow rates $q(t)$ and $Q(t)$:

$$q(t) = \frac{2c\gamma}{3\mu h\,(\ell(t)) \int_0^{\ell(t)} [h(z)]^{-3}\,\mathrm{d}z} \quad \text{(2D)} \quad \text{or} \quad Q(t) = \frac{\pi c\gamma}{8\mu h\,(\ell(t)) \int_0^{\ell(t)} [h(z)]^{-4}\,\mathrm{d}z} \quad \text{(3D)}. \tag{2.3}$$

We can then determine the speed of movement of the meniscus $u_m = \mathrm{d}\ell/\mathrm{d}t = q(t)/2h$ (two-dimensional) or $u_m = \mathrm{d}\ell/\mathrm{d}t = Q(t)/\pi h^2$ (three-dimensional), where $h(z)$ is evaluated at the meniscus location $z = \ell(t)$ so that

$$\frac{\mathrm{d}\ell}{\mathrm{d}t} = \frac{c\gamma}{3\mu h\,(\ell(t))^2 \int_0^{\ell(t)} [h(z)]^{-3}\,\mathrm{d}z} \quad \text{(2D)} \quad \text{or} \quad \frac{\mathrm{d}\ell}{\mathrm{d}t} = \frac{c\gamma}{8\mu h\,(\ell(t))^3 \int_0^{\ell(t)} [h(z)]^{-4}\,\mathrm{d}z} \quad \text{(3D)}. \tag{2.4}$$

These equations effectively serve as a generalization of the usual imbibition equation for invasion into a structured (shaped) solid of any cross-sectional shape. It remains to solve the equation for $\ell(t)$ for different choices of the channel shape $h(z)$. We will develop three particular cases: the classic example of a straight axisymmetric channel, the wedge (or cone) geometry, and a case with a power-law change of shape.

2.1. Straight channels

For the familiar three-dimensional case of a straight axisymmetric channel of radius $h_0 = $ constant, put into contact with a wetting liquid of contact angle θ_e (imbibition requires $\theta_e < \pi/2$), we have $c = 2\cos\theta_e$, i.e. the curvature at the meniscus is $2\cos\theta_e/h_0$. Thus, (2.4) simplifies to

$$\frac{\mathrm{d}\ell}{\mathrm{d}t} = \frac{\gamma\cos\theta_e h_0}{4\mu\ell} \quad \text{or} \quad \ell(t) = \left(\frac{\gamma\cos\theta_e h_0 t}{2\mu}\right)^{1/2}, \tag{2.5}$$

where we have also taken $\ell(0) = 0$. This equation is exactly the result obtained by Lucas (1918) and Washburn (1921). We note that since the meniscus is moving, for systems with significant contact angle hysteresis, θ_e should be replaced by the receding contact angle θ_r.

2.2. Invasion into a wedge (two-dimensional) or a cone (three-dimensional)

2.2.1. Analytical solution

Next we consider a wedge or a cone of opening angle α as defined in figure 1(a) (the lubrication approximation requires $\alpha \ll 1$ in order to link the local shape to the permeability). If θ_e is the contact angle of the liquid on the solid walls ($\theta_e < \pi/2$), the curvature of the meniscus can be written as $\kappa = c/h$ with $c = \cos(\theta_e + \alpha)$ for a wedge and $c = 2\cos(\theta_e + \alpha)$ for a cone. In both cases, the shape of the channel is given by

$$h(z) = h_0 + \alpha z. \tag{2.6}$$

Equations (2.4) yield

$$\frac{d\ell}{dt}\left(\left(1+\frac{\alpha\ell}{h_0}\right)^2-1\right)=\frac{2c\gamma\alpha}{3\mu}\quad\text{(2D)}\quad\text{or}\quad\frac{d\ell}{dt}\left(\left(1+\frac{\alpha\ell}{h_0}\right)^3-1\right)=\frac{3c\gamma\alpha}{8\mu}\quad\text{(3D)}.$$

(2.7)

It is then convenient to identify two dimensionless parameters

$$L=\frac{\alpha\ell}{h_0}\quad\text{and}\quad T=\frac{c\gamma\alpha^2}{\mu h_0}t$$

(2.8)

which simplify (2.7) to

$$\frac{dL}{dT}((1+L)^2-1)=\frac{2}{3}\quad\text{(2D)}\quad\text{or}\quad\frac{dL}{dT}((1+L)^3-1)=\frac{3}{8}\quad\text{(3D)}.$$

(2.9)

Integrating with $L(0)=0$ and simplifying yields

$$L^3+3L^2=2T\quad\text{(2D)}\quad\text{or}\quad 2L^4+8L^3+12L^2=3T\quad\text{(3D)}.$$

(2.10)

At short times these equations yield the familiar 'diffusive' result $L\propto T^{1/2}$. However, at longer times ($T\gg 1$), $L\propto T^{1/3}$ (two-dimensional) or $L\propto T^{1/4}$ (three-dimensional), which is much slower. The cross-over between these two different dynamics occurs for $L\simeq 1$ or $\ell\simeq h_0/\alpha$.

2.2.2. *Interpretation*

In this section, we give a qualitative order-of-magnitude description to rationalize the relationship between the shape and the power-law exponents. We will consider the conical axisymmetric three-dimensional shape, but the same arguments apply to the two-dimensional case.

At short times, $h(z)\simeq h_0$, the half-width at the orifice. The viscous effects are $\mu u/k$ where $k=O(h_0^2)$. Also, the pressure drop $\Delta p=O(\gamma/h_0)$ occurs over a length $\ell(t)$. Thus, as $u=d\ell/dt$, we have $\ell\simeq(\gamma h_0 t/\mu)^{1/2}$ as expected for a nearly straight channel.

At long times, where $\ell>h_0/\alpha$, so that $h(\ell)\simeq\alpha\ell$, the physical balances are modified. The pressure drop $\Delta p=O(\gamma/h(\ell))$ varies monotonically from the reservoir to the meniscus, but most of the pressure drop occurs over the shorter length h_0/α. The typical velocity u_0, in this part of the tube, is set by the Darcy equation: $\mu u_0/k\simeq\Delta p/(h_0/\alpha)$ or $u_0\simeq\gamma h_0/\mu\ell$. Finally, the movement of the meniscus is given by mass conservation $u(\ell)h(\ell)^2=u_0 h_0^2$, which, with $u=d\ell/dt$, yields $\ell(t)\simeq(\gamma h_0^3 t/\mu\alpha^2)^{1/4}$, in agreement with (2.10). Similar ideas, combining the 'confinement' or localization of most of the pressure drop, Darcy's law, and mass conservation to yield the movement of the meniscus, apply to other shapes.

3. Experiments

We have observed experimentally a deviation from the 'diffusive' law of imbibition by considering a conical geometry. We have worked with two sets of cones. The first set is commercial plastic pipet tips with a typical opening angle of $4°$ and an initial radius varying from $200-250\,\mu m$. The second set of cones is fabricated by pulling glass capillaries with a pipette puller (Sutter Instrument). This technique allows the formation of cones with controlled opening angles and initial radii. The opening angle can vary from $1°$ to several degrees and the initial radius can be as small as $5\,\mu m$. Images of these cones are shown in figure 2.
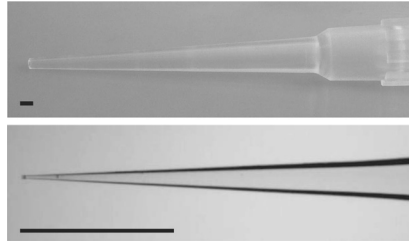
FIGURE 2. Images of the two sets of cones used for the experiments. The first cone is a commercial plastic pipet tip (upper image), whereas the second cone is made by pulling a glass capillary tube (lower image). The scale bars represent 1 mm.
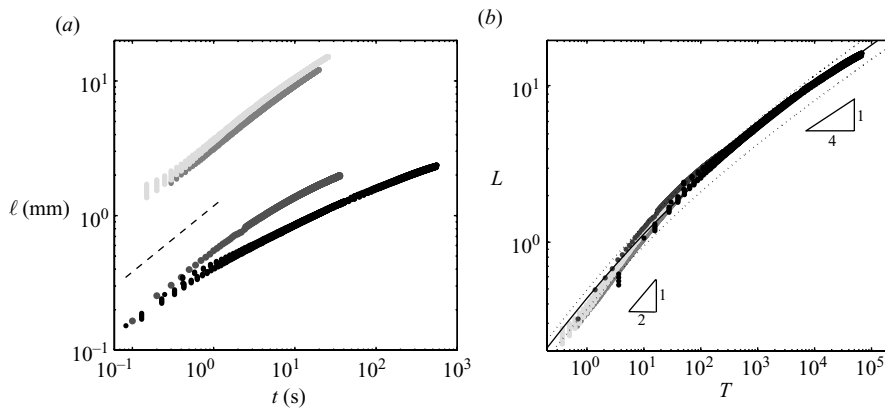

FIGURE 3. (*a*) Log-log plot of the position of the meniscus inside the conical tubes as a function of time. The dashed line has a slope of $1/2$ and represents the classical diffusive response. Four different experiments are reported: the two upper sets of results were obtained with commercial cones from pipet tips ($h_0 = 200\,\mu\mathrm{m}$, $\alpha = 3.8°$ and $h_0 = 225\,\mu\mathrm{m}$, $\alpha = 4.2°$), whereas the two lower series correspond to experiments with conical micro-pipets ($h_0 = 5\,\mu\mathrm{m}$, $\alpha = 4.8°$ and $h_0 = 5\,\mu\mathrm{m}$, $\alpha = 1.0°$). Experiments were performed with silicone oil of viscosity 0.1 Pa s and surface tension of $2 \times 10^{-2}\,\mathrm{N\,m^{-1}}$. (*b*) Rescaling of the data with the dimensionless parameters defined in (2.8). The continuous curve corresponds to equation (2.10). No fitting parameters have been used. The two dashed curves take into account the error bars on L and T, which are about 25%. Two regimes are visible: at short times, the motion follows $L \propto T^{1/2}$, whereas at longer times, the motion is much slower and follows $L \propto T^{1/4}$.

The experiment consists of putting the conical tubes into contact with a reservoir of silicone oil ($\mu \simeq 0.1\,\mathrm{Pa\,s}$, $\gamma \simeq 2 \times 10^{-2}\,\mathrm{N\,m^{-1}}$ and $\theta_e \simeq 0°$) and measuring the time-dependent position of the meniscus. To eliminate gravitational effects, we place the tubes horizontally. With the larger cones, we verified that the meniscus remained axisymmetric and was not deformed by gravity.

In figure 3(*a*), we report, in a logarithmic representation, the meniscus position ℓ as a function of time, for four different experiments with varying opening angles and initial radii. For all of the cones, the results illustrate clearly that the movement of the meniscus first follows the classical diffusive law (the dashed line, of slope $1/2$, is a guide for the eyes). However, deviations are observed at long times and correspond to slowing down of the imbibition relative to the diffusive expectation.

In order to compare these experimental results to the theoretical predictions given by (2.10), we used the dimensionless variables defined in (2.8) and re-plotted our data with these parameters; all properties were measured so that there are no fitting

parameters. This representation is displayed in figure 3(b). We observe that all of the data, for the four different experiments, collapse onto a single curve and that this curve is well fitted for all times by (2.10), which is represented by the continuous curve.

Two regimes can be then distinguished in the experiments: at short times, $\ell \propto t^{1/2}$, whereas at long times, $\ell \propto t^{1/4}$. The transition between these two regimes occurs when $L \simeq 1$, i.e. at an axial distance of the order of h_0/α (recall that h_0 is the opening radius and α half of the opening angle of the cone). The theory (equation (2.10)) predicts the cross-over for $L = \sqrt{6}$ and $T = 24$ in three dimensions, which is very close to the experimental results (figure 3b). Thus, this second regime can only be seen when h_0/α is small enough relative to the length of the cone: this limit is clearly achieved for the micro-pipet shown in figure 2(b) where $h_0 \simeq 5\,\mu\text{m}$ and $\alpha \simeq 5°$. Imbibition in this pipet corresponds to the longest time dynamics in figure 3. This result shows that deviations from 'Washburn's' law are to be expected by simply modifying the shape along the length of a sufficiently long channel.

4. Invasion into a power-law-shaped channel

It is also useful to consider the general case of a power-law-shaped profile defined as

$$h(z) = h_0 + \alpha z^n, \qquad (4.1)$$

with h_0 being half of the height of the opening. Now α is a parameter whose dimensions depend on the exponent n (the one-dimensional lubrication approach requires $n \geqslant 1$).

The meniscus motion is then determined from (2.4) for the two-dimensional and the three-dimensional cases:

$$\frac{\mathrm{d}\ell}{\mathrm{d}t}\left(1+\frac{\alpha}{h_0}\ell^n\right)^2 \int_0^{\ell(t)} \left(1+\frac{\alpha}{h_0}z^n\right)^{-3} \mathrm{d}z = \frac{c(\ell)\gamma h_0}{3\mu} \quad (2\mathrm{D}), \qquad (4.2a)$$

$$\frac{\mathrm{d}\ell}{\mathrm{d}t}\left(1+\frac{\alpha}{h_0}\ell^n\right)^3 \int_0^{\ell(t)} \left(1+\frac{\alpha}{h_0}z^n\right)^{-4} \mathrm{d}z = \frac{c(\ell)\gamma h_0}{8\mu} \quad (3\mathrm{D}). \qquad (4.2b)$$

In the general case, c is not constant but depends on the position of the meniscus inside the tube

$$c(\ell) = \cos\left(\theta_e + \arctan\left(\frac{\mathrm{d}h}{\mathrm{d}z}(\ell)\right)\right) \ (2\mathrm{D}) \ \text{ or } \ c(\ell) = 2\cos\left(\theta_e + \arctan\left(\frac{\mathrm{d}h}{\mathrm{d}z}(\ell)\right)\right) \ (3\mathrm{D}), \qquad (4.3)$$

where θ_e is the contact angle of the liquid on the walls of the solid ($\theta_e < \pi/2$). Since the cosine is bounded and generally $c = O(1)$, we will make the approximation that $c(\ell) = \text{constant} = c_0$. The details of this assumption, in the particular case where $\theta_e \ll 1$, are given in the Appendix. Accordingly, we can again identify two dimensionless parameters:

$$L = \left(\frac{\alpha}{h_0}\right)^{1/n} \ell \quad \text{and} \quad T = \frac{c_0\gamma h_0}{\mu}\left(\frac{\alpha}{h_0}\right)^{2/n} t, \qquad (4.4)$$

which simplify (4.2) into

$$\frac{\mathrm{d}L}{\mathrm{d}T}(1+L^n)^2 \int_0^{L(T)} (1+Z^n)^{-3} \, \mathrm{d}Z = \frac{1}{3} \quad (2\mathrm{D}), \qquad (4.5a)$$

$$\frac{\mathrm{d}L}{\mathrm{d}T}(1+L^n)^3 \int_0^{L(T)} (1+Z^n)^{-4}\,\mathrm{d}Z = \frac{1}{8} \quad \text{(3D).} \tag{4.5b}$$

These equations can be solved analytically (e.g. with *Maple*). The case $n=1$ corresponds to the previously detailed shape of a wedge or a cone (§2.2). We will detail the case $n=2$, which also has a simple solution, before giving the two asymptotic limits for any values of n.

4.1. $n=2$: invasion into a parabolically shaped channel

The case $n=2$ corresponds to capillary-driven invasion of a parabolically changing gap as shown in figure 1(*b*). This flow can be observed in two dimensions with two closely spaced cylinders of radius $R=1/2\alpha$. Integrating (4.5) with the condition $L(0)=0$ yields

$$9L^2(3+L^2)+(45+30L^2+9L^4)L\arctan(L)-12\ln(1+L^2) = 40T \quad \text{(2D),} \tag{4.6a}$$

$$\begin{aligned} 87L^2+58L^4+15L^6-24\ln(1+L^2) \\ +(105+105L^2+63L^4+15L^6)L\arctan(L) = 42T \quad \text{(3D).} \end{aligned} \tag{4.6b}$$

For short times, equations (4.6) again yield the diffusive result $L \propto T^{1/2}$. For long times, $T \gg 1$, which correspond to $L \gg 1$, we can approximate these equations by

$$\frac{9\pi}{2}L^5 \sim 40T \quad \text{(2D)} \quad \text{and} \quad \frac{15\pi}{2}L^7 \sim 42T \quad \text{(3D),} \tag{4.7}$$

which shows that asymptotically $L \propto T^{1/5}$ in two dimensions and $L \propto T^{1/7}$ in three dimensions. These results differ from the ones found previously for a wedge or a cone and also reflect a significant slowing down of the invasion dynamics. The cross-over time occurs on a length scale $L \simeq 1$ which corresponds to $\ell \simeq \sqrt{h_0/\alpha}$ or $\ell \simeq \sqrt{Rh_0}$.

4.2. Asymptotic limits

In the general case, we can detail the two asymptotic limits of equations (4.5).

(i) At short times, which corresponds to $L \ll 1$, $\int_0^{L(T)}(1+Z^n)^{-(d+1)}\,\mathrm{d}Z \simeq L(t)$, where d is the chosen dimension ($d=2$ or 3). Thus, equations (4.5) simplify into

$$L\frac{\mathrm{d}L}{\mathrm{d}T} \simeq \text{constant.} \tag{4.8}$$

This equation leads to the classical 'diffusive' law $L \propto T^{1/2}$, valid at short times.

(ii) At long times, or when $L \gg 1$, $(1+L^n) \simeq L^n$ and the integrals $\int_0^{L(t)}(1+Z^n)^{-(d+1)}\,\mathrm{d}Z$ ($d=2$ or 3) can be approximated by $\int_0^{\infty}(1+Z^n)^{-(d+1)}\,\mathrm{d}Z$, which converge if $n>1/3$ in two dimensions or $n>1/4$ in three dimensions (this criterion is always satisfied in the lubrication approximation, which requires $n \geqslant 1$). Thus, we define

$$A(n) = \int_0^{\infty}(1+Z^n)^{-3}\,\mathrm{d}Z = \frac{\pi}{2}\frac{(2n-1)(n-1)}{n^3\sin(\pi/n)} \quad \text{with} \quad n>\frac{1}{3}, \tag{4.9a}$$

$$B(n) = \int_0^{\infty}(1+Z^n)^{-4}\,\mathrm{d}Z = \frac{\pi}{6}\frac{(3n-1)(2n-1)(n-1)}{n^4\sin(\pi/n)} \quad \text{with} \quad n>\frac{1}{4}. \tag{4.9b}$$

Thus, equations (4.5) become

$$A(n)L^{2n}\frac{\mathrm{d}L}{\mathrm{d}T} \sim \frac{1}{3} \quad \text{(2D)} \quad \text{or} \quad B(n)L^{3n}\frac{\mathrm{d}L}{\mathrm{d}T} \sim \frac{1}{8} \quad \text{(3D),} \tag{4.10}$$
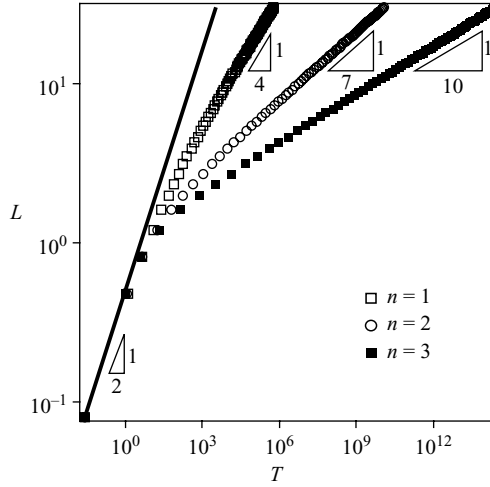
FIGURE 4. Log-log representation of analytical solutions of (4.5b) for three values of n in the three-dimensional axisymmetric geometry. L and T are, respectively, the dimensionless position of the meniscus and time. The classical 'diffusive' law $L \propto T^{1/2}$ is represented by the continuous line. The more diverging the geometry the slower the dynamics is at long times.

which yields the power laws

$$L^{2n+1} \sim \frac{2n+1}{3A(n)}T \quad \text{(2D)} \quad \text{or} \quad L^{3n+1} \sim \frac{3n+1}{8B(n)}T \quad \text{(3D)}. \qquad (4.11)$$

These equations predict long-time behaviours. The results $L \propto T^{1/3}$ and $L \propto T^{1/4}$ previously obtained for the case $n = 1$ can be recovered from these equations. The cross-over between these two limits occurs for $L \simeq 1$, i.e. $\ell \simeq (h_0/\alpha)^{1/n}$. In figure 4, three different solutions of (4.5b) have been represented for the three-dimensional axisymmetric geometry. For each value of n, two asymptotic limits are clearly visible: the first regime, of slope $1/2$, is common for all of the curves. The second regime, given by (4.11), clearly depends on the value of n: the more diverging the geometry, the slower the dynamics become at long times.

5. Concluding remarks

Deviations from the well-established diffusive imbibition of porous media have been provided, both theoretically and experimentally, for channels with axial variations in shape. Experiments have been performed with conical geometries and very good agreement has been observed with quasi-steady viscous flow theory. We have shown that two regimes can be successively observed: at short times $\ell \propto t^{1/2}$, whereas $\ell \propto t^{1/4}$ at longer times. Our work shows that a small monotonic modification of the shape of a channel leads to a significant change in the dynamics of invasion.

Nevertheless, as is well known, the diffusive dynamics also apply to the case of random porous media where the channel cross-section varies continuously from pore to pore and has a well-defined average value that is independent of position. Similar to our results for channels of slowly varying shape (or permeability), we expect, for porous media with slow and monotonic variations of the permeability, that the imbibition rate will depend on the spatial variation of the permeability.

We close with a comment on the history of this subject of capillary invasion. As indicated in the introduction, the diffusive dynamics of the wetting front is often referred to as the 'Washburn equation.' Nevertheless, there are several papers that precede Washburn's 1921 paper, as others have occasionally referenced. For example, the diffusive imbibition result is sometimes mentioned as the 'Lucas–Washburn equation' in reference to a paper by Lucas (1918). In fact, Bell & Cameron (1906) described the penetration of a liquid inside capillary spaces and found exactly the same scaling result, which is that the penetration distance increases as the square root of time. Bell & Cameron compared this prediction to experiments with capillary tubes brought into contact with different liquids and found good agreement. They also looked at the imbibition of porous media such as filter paper and dry soils and found similar dynamics. We note that on the last page of Lucas's paper, the paper of Bell & Cameron is referenced with a comment that although the latter obtained the scaling result $\ell \propto t^{1/2}$, Lucas established the form of the prefactor. We thus propose for the future to refer to these capillary-driven flows as the 'BCLW imbibition' in order to recognize the original contributions of Bell & Cameron in 1906, Lucas in 1918, and Washburn in 1921.

Appendix. The assumption $c \simeq$ constant in the condition on the pressure jump at the interface

As noted in §4, the coefficient c depends slightly on the position of the meniscus inside the tube through the equation

$$c(\ell) \propto \cos\left(\theta_e + \arctan\left(\frac{\mathrm{d}h}{\mathrm{d}z}(\ell)\right)\right), \tag{A 1}$$

Let us consider the profile $h(z) = h_0 + \alpha z^n$, with $n > 1$. The lubrication theory requirement ($\mathrm{d}h/\mathrm{d}z \ll 1$) leads to the simplification $\arctan(\mathrm{d}h/\mathrm{d}z(\ell)) \simeq \mathrm{d}h/\mathrm{d}z(\ell) = n\alpha\ell^{n-1}$. If we now consider a completely wetting case with $\theta_e \ll 1$,

$$c \propto 1 - \frac{n^2}{2}\alpha^2\ell^{2n-2} + \cdots \tag{A 2}$$

The approximation $c \simeq$ constant can then hold if $n^2\alpha^2\ell^{2n-2} \ll 1$, i.e.

$$\ell \ll \left(\frac{1}{\alpha n}\right)^{1/(n-1)}. \tag{A 3}$$

On the other hand, we know that the cross-over time between the two asymptotic limits occurs on a length scale $L \simeq 1$ or $\ell \simeq (h_0/\alpha)^{1/n}$. Thus, the approximation $c \simeq$ constant remains valid if

$$\left(\frac{h_0}{\alpha}\right)^{1/n} \ll \left(\frac{1}{\alpha n}\right)^{1/(n-1)} \quad \text{or} \quad h_0 \ll (\alpha n^n)^{1/(1-n)}. \tag{A 4}$$

We assume the cases considered here to be under this condition.

REFERENCES

BELL, J. M. & CAMERON, F. K. 1906 The flow of liquids through capillary spaces. *J. Phys. Chem.* **10**, 658–674.

BICO, J., TORDEUX, C. & QUÉRÉ, D. 2001 Rough wetting. *Europhys. Lett.* **55**, 214220.

COURBIN, L., DENIEUL, E., DRESSAIRE, E., ROPER, M., AJDARI, A. & STONE, H. A. 2007 Imbibition by polygonal spreading on microdecorated surfaces. *Nature Materials* **06**, 661–664.

DULLIEN, F. A. L. 1979 *Porous Media. Fluid Transport and Pore Structure*. Academic.

DUSSAUD, A. D., ADLER, P. M. & LIPS, A. 2003 Liquid transport in the networked microchannels of the skin surface. *Langmuir* **19**, 7341–7345.

ERICKSON, D., LI, D. & PARK, C. B. 2002 Numerical simulations of capillary-driven flows in nonuniform cross-sectional capillaries. *J. Colloid Interface Sci.* **250**, 422430.

KROTOV, V. V. & RUSANOV, A. I. 1999 *Physicochemical Hydrodynamics of Capillary Systems*. Imperial College Press.

LUCAS, V. R. 1918 Ueber das zeitgesetz des kapillaren aufstiegs von flüssigkeiten. *Kolloid Zeistschrift* **23**, 15–22.

POLZIN, K. A. & CHOUEIRI, E. Y. 2003 A similarity parameter for capillary flows. *J. Phys.* D: *Appl. Phys.* **36**, 3156–3167.

ROMERO, L. A. & YOST, F. G. 1996 Flow in an open channel capillary. *J. Fluid Mech.* **322**, 109–129.

RYE, R. R., YOST, F. G. & O'TOOLE, E. J. 1998 Capillary flow in irregular surface grooves. *Langmuir* **14**, 3937–3943.

WARREN, P. B. 2004 Late stage kinetics for various wicking and spreading problems. *Phys. Rev.* E **69**, 041601.

WASHBURN, E. W. 1921 The dynamics of capillary flow. *Phys. Rev.* **17**, 273–283.

WEISLOGEL, M. M. & LICHTER, S. 1998 Capillary flow in an interior corner. *J. Fluid Mech.* **373**, 349–378.

YOUNG, W. B. 2004 Analysis of capillary flows in non-uniform cross-sectional capillaries. *Colloids and Surfaces* A: *Physicochem. Engng Aspects* **234**, 123128.